

ANALYSIS OF FLUX DECLINE DURING MICELLAR ENHANCED ULTRAFILTRATION FOR REMOVAL OF CRYSTAL VIOLET DYE FROM AQUEOUS SOLUTION

Report submitted in partial fulfillment of the requirement for the
Degree of
Bachelor of Technology
In
Biochemical Engineering

By
Nikhil Kapoor
(Roll No: 40916100418)

Under the supervision of
Prof. Biswajit Sarkar



UNIVERSITY SCHOOL OF CHEMICAL TECHNOLOGY
Guru Gobind Singh Indraprastha University, Delhi
June 2022

CERTIFICATE

This is to certify that the Report entitled “ANALYSIS OF FLUX DECLINE DURING MICELLAR-ENHANCED ULTRAFILTRATION FOR REMOVAL OF CRYSTAL VIOLET DYE FROM AQUEOUS SOLUTION” which is submitted by NIKHIL KAPOOR in partial fulfillment of the requirements for the award of degree B.Tech. in Biochemical Engineering to USCT, GGSIP University, Dwarka, New Delhi is a record of the candidate own work carried out by him under my supervision. The matter embodied in this report is original and has not been submitted for an award of any other degree.

Date -

Supervisor - Dr. Biswajit Sarkar
Professor, USCT

ACKNOWLEDGEMENT

Working on the project on “ANALYSIS OF FLUX DECLINE DURING MICELLAR-ENHANCED ULTRAFILTRATION FOR REMOVAL OF CRYSTAL VIOLET DYE FROM AQUEOUS SOLUTION” was a source of immense knowledge to me. Besides doing experiments on removing harmful dyes from aqueous solution, I could also get a good exposure of developing codes and working on modelling software.

Further, I want to express my special gratitude to Dr. Biswajit Sarkar, Professor of University School Chemical Technology, for guiding me throughout the project. Without his supervision, the project would have been incomplete. I would also like to thank the University for giving me an opportunity to work on this project.

Nikhil Kapoor
40916100418

OBJECTIVE

- To investigate the removal of Crystal Violet from aqueous solution by micellar-enhanced ultrafiltration with Rhamnolipid as a bio surfactant.
- To conduct dead-end ultrafiltration. To evaluate the performance of micellar-enhanced ultrafiltration for the removal of Crystal Violet
- Development of model for prediction of permeate flux and analyse the flux decline due to cake formation
- To observe the effects of flux decline at various operating conditions such as transmembrane pressure, Specific Cake Resistance on flux profile and Rejection Rate of RHL Vesicles.

ABSTRACT

The continuous dumping of dyes into the water by industries has led to a considerable damage to the environment. These dyes are highly acid and toxic in nature. To safeguard the environment, it is the need of an hour to remove these dyes from the wastewater. To achieve this, Micellar Enhanced Ultrafiltration experiments were performed using Rhamnolipid in a stirred cell for the removal of crystal violet dye from aqueous solution. This project deals with the interpretation of declining flux during these experiments. The influence of various operating conditions on the transient profiles of permeate flux was investigated. The predicted results show good agreement with the experimental data. The estimated model parameters in this study would help in the design and scaling up of such MEUF process.

Table of Contents

INTRODUCTION	7
VARIOUS TECHNIQUES OF DYE REMOVAL.....	8
MEMBRANES.....	10
MICELLAR-ENHANCED ULTRAFILTRATION	11
MATERIALS AND METHODS	12
THEORY.....	14
PROCEDURE	17
CLEANING OF MEMBRANE	17
VARIOUS PARAMETRIC VALUES.....	18
RESULT AND DISCUSSION	19
CONCLUSION	28
REFERENCES.....	29

INTRODUCTION

A dye is a substance that is used to impart color to textiles, cosmetics, paper, leather, rubber and other materials. These colorants originate from plants and from insects, fungi and lichens. These colored substances chemically bond to the substrate to which they are being applied. Exposing the material to washing, heat, light and other factors are not enough readily altering the coloring.

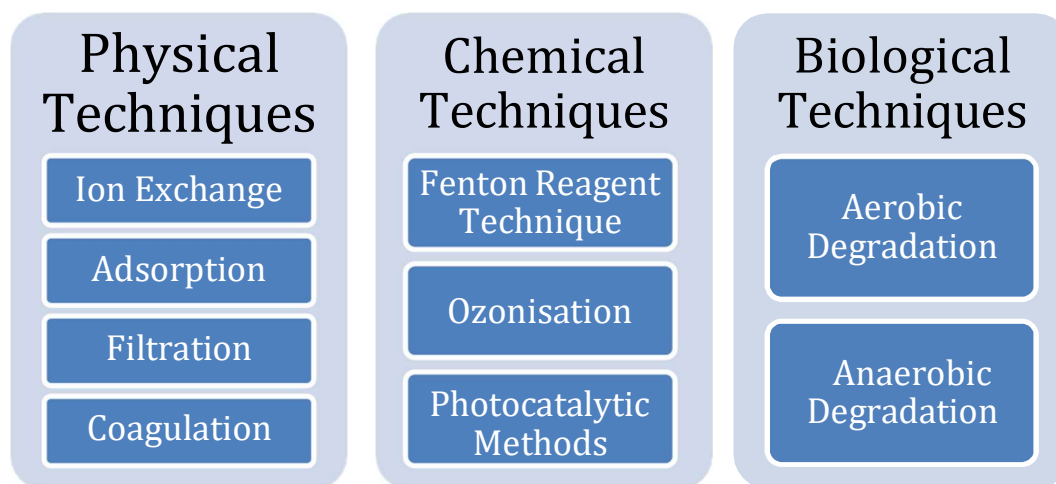


However, these dyes are highly soluble in water. Hence, the wastewater produced by industries may contain highly acidic dyes. As these dye molecules have highly complex structures, they are highly troublesome in the purification processes. These dyes are highly hazardous to the environment and even very minute number of dyes are quite undesirable.



These dyes are reflected in the bright color of the water, making it look un-attractive and is also responsible for disturbing life processes in water. Most dyes do not undergo biodegradation, deteriorate the penetration of light into the water and inhibit photosynthesis, increase chemical and biological demand for oxygen. Some dyes exhibit toxic and even cancer genic as well as mutagenic action toward living organisms and therefore they should be removed prudently.

VARIOUS TECHNIQUES OF DYE REMOVAL



Ion Exchange Method

Ion exchange is a very versatile and effective tool for treating of aqueous hazardous wastes including dyes. The role of ion exchange in dye effluent treatment is to reduce the magnitude of hazardous load by converting them into a form in which they can be reused, leaving behind less toxic substances in their places, or to facilitate ultimate disposal by reducing the hydraulic flow of the stream bearing toxic substances.

Adsorption

The simplest and cheapest among the other processes, it is most favorable amongst all. Adsorption is defined as the concentration of materials on the surface of a solid bodies. Adsorption is a surface phenomenon that deals primarily with the usage of surface forces. When a solution having absorbable solute, known as an adsorbate, comes into contact with a solid, called an adsorbent, with highly porous surface structure liquid-solid intermolecular forces of attraction cause the solute to be concentrated on the solid surface.

Filtration

It is one of the most efficient methods of dye removal regardless of the type of dye. Process filtration involves separating the constituents of a liquid-solid mixture by passing them through a filter medium. Generally, this process requires high pressure and concentrated sludge may also be formed on the filter medium.

Fenton Reagent Technique

Fenton's reagent is a solution of hydrogen peroxide (H_2O_2) with ferrous iron as a catalyst that is used to oxidize contaminants or wastewaters. This reactant is an attractive oxidative system for wastewater treatment because iron is a very abundant and non-toxic element and hydrogen peroxide is easy to handle and environmentally safe. This reactant is an attractive oxidative system for wastewater treatment because iron is a very abundant and non-toxic element and hydrogen peroxide is easy to handle and environmentally safe. However, it requires high operational costs and a by-product may also be formed.

Ozonisation

Ozonisation is a chemical water treatment technique based on the infusion of ozone into water. Ozone is a gas composed of three oxygen atoms (O_3), which is one of the most powerful oxidants. Ozonisation is a type of advanced oxidation process, involving the production of very reactive oxygen species able to attack various organic compounds. However, with the low stability of the oxidant, a hazardous by-product may be formed.

Photocatalytic Methods

Photo catalysis is a promising wastewater treatment method, which is used to remove dyes under light irradiation in the presence of a photo catalyst. The photo catalysis process has huge potential as a tertiary treatment method for the degradation of numerous organic compounds and dyes in wastewater. However, this process will become more economical and sustainable once solar-light-driven photo catalysis techniques are established.

Biological Methods

Biological degradation (Bioremediation) is an economically feasible, environmentally- friendly method that generates less volume of sludge compared with other techniques. It causes the degradation of synthetic dyes to a comparatively less toxic inorganic compound because of the breakdown of bonds (i.e., chromophore group) and finally helps in the removal of color. While the efficiency of oxidizable material is 90%, however the dye comes out to have very low biodegradability. It can be done either under aerobic or anaerobic conditions.

MEMBRANES

A membrane is a thin sheet that forms a barrier. It is highly selective. it allows some material to pass through it whereas restricts the entry of others. The degree of selectivity of a membrane depends on the membrane pore size. Depending on the pore size, they can be classified as microfiltration (MF), ultrafiltration (UF), Nanofiltration (NF) and reverse osmosis (RO) membranes.

Type	Pore Size (in μm)	Pressure Range (in kPa)
Microfiltration	0.08 - 2	7 - 100
Ultrafiltration	0.005 -2	70 - 700
Nanofiltration	0.002	500 - 1500
Reverse Osmosis	0.001	850 – 7000

The most widely used membranes in dye industries are Nano-filtration and reverse osmosis membranes-

Nanofiltration Membranes

Nanofiltration membranes use nanometer sized through-pores that pass through the membrane. Nanofiltration is used for the removal of selected dissolved constituents from wastewater. Nanofiltration has been primarily developed as a membrane softening process that offers an alternative to chemical softening. It has a wide range of applications in the dye and textile industries-

- Dye Concentration – By allowing salts and water to pass through an NF membrane, Nanofiltration can be a practical alternative for the concentration and desalination of dyes used in the textile industry.
- Dye Penetrant Removal – Nanofiltration is widely applied in the recovery of dye to meet discharge regulations after penetrant testing with fluorescent dyes.
- Optical Brightening Agent (OBA) Concentration & Desalination – Optical brightening agents can enhance the appearance of colors by increasing the amount of light reflected. To reduce operating costs, Nanofiltration can be applied to concentrate the optical brightening agents for reuse in the textile industry.

Reverse Osmosis Membranes

Also known as hyperfiltration, Reverse osmosis (RO) is a water purification process that uses a partially permeable membrane to separate ions, unwanted molecules and larger particles from water. In reverse osmosis, an applied pressure is used to overcome the osmotic pressure. Reverse Osmosis has been successfully applied on a large scale throughout the world for treating of effluent and the polluted water. Reverse osmosis process for water purification does not require thermal energy. High pressure pumps regulates the flow-through reverse osmosis systems. The recovery of purified water depends upon various factors, including membrane sizes, membrane pore size, temperature, operating pressure, and membrane surface area. The ability of RO membranes to remove both organic and inorganic compounds has made it attractive for treating of contaminated drinking water supplies. Reverse osmosis processes can simultaneously remove hardness, color, many kinds of bacteria and virus, and organic contaminants such as agricultural chemicals and trihalomethane precursors.

MICELLAR-ENHANCED ULTRAFILTRATION

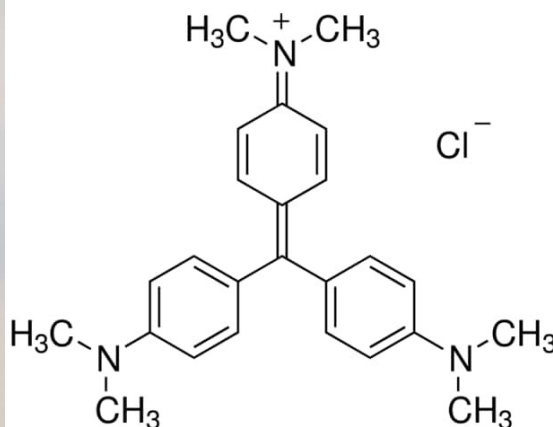
Micellar-enhanced ultrafiltration (MEUF) is a surfactant based separation technique which can be used to remove metal ions or dissolved organics from water. It is effective and economical to remove dye and reuse water for further processing, and has been extensively investigated in the past three decades.

In the MEUF process, surfactant with a higher concentration than the critical micelle concentration is added to the aqueous dye solution. The surfactant molecules form micelles, whose interior hydrophobic core can solubilize the dye molecules and its hydrophilic surface adsorbs counter ions due to electrostatic interactions. The micellar solution is then filtered through an ultrafiltration membrane with pore sizes smaller than those of the micelle-dye complexes. Ultrafiltration membrane can thus remove the micelles containing the solubilized dyes, highly purified (almost dye free) permeate stream can be obtained. This technique offers the high selectivity of NF and RO, and the high flux of ultrafiltration at relatively low operating pressures.

The MEUF process has been successfully used as a replacement of the highly energy-consuming Nanofiltration and Reverse Osmosis processes to remove dyes from waste-water.

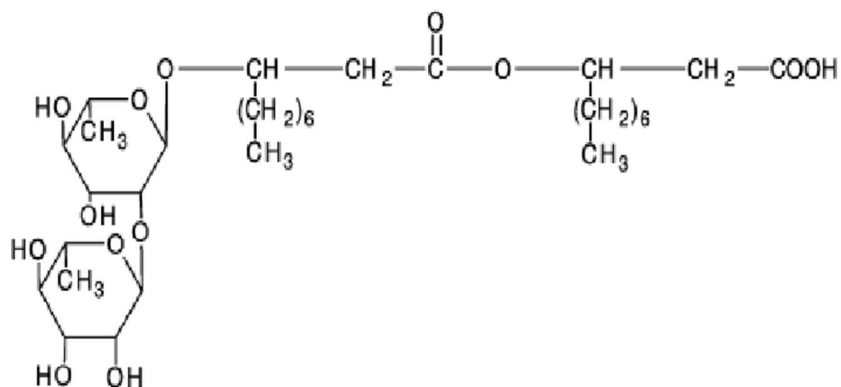
MATERIALS AND METHODS

- Filtrate used – Crystal Violet ($C_{25}N_3H_{30}Cl$)



Also known as Gentian Violet, Hexamethyl Pararosaniline Chloride is a triarylmethane dye used as a histological stain and in Gram's Method to differentiate between Gram-positive and gram-negative bacteria. It is widely used in textile industry as a coloring agent and is known for its mutagenic and mitotic poisoning nature.

- Surfactant Used – Rhamnolipid ($C_{32}H_{58}O_{13}$)



Rhamnolipid is a class of bio-surfactants, which contain rhamnose as the sugar moiety linked to β -hydroxylated fatty acid chains. They are a class of glycolipids produced by *Pseudomonas aeruginosa*.

➤ Equipment used – Stirred Cell Batch Membrane Setup



The complete set up consists of the following –

- Pressure Gauge – This is used to set up the desired pressure during the experiment
- Stirrer – The mechanical agitating device is used to maintain the flow rate of the concentrated dye till it completely exists from the vessel
- Gas Cylinder – This is used to provide pressure for the system to work
- Tachometer – Also known as the RPM Gauge, this instrument is used for measuring the rotation speed of the stirrer
- Joining pipes, stands to keep the collecting tubes, etc.

The setup was used to get the experimental readings of the flux with respect to the time

➤ Membrane Used – Ultrafiltration Membrane



Complete readings were obtained using an ultrafiltration membrane. Round-shaped pieces were cut from the membrane sheath.

THEORY

In membrane separation, crystal violet is pumped from a process tank at a moderate and constant pressure and rapid flow through a membrane. Large molecules are blocked at the membrane surface. The compounds that do not pass through the membrane are referred to as the retentate. The water-like solutions that pass through the membrane are referred to as the "permeate".

Flux Rate

Also known as the Permeate Rate, it is defined as the rate at which the permeate flows through the membrane per unit area per unit time.

$$\frac{dV_r}{dt} = -V_w A$$

(4)

A - Effective membrane area

V_r - Retentate Volume

V_w - Volume of permeate collected in sampling time t

Theoretical Removal Efficiency

The rejection rate is defined as the amount of feed that freely passes through the membrane. The observed rejection for any solute was calculated as –

$$R_o^s = 1 - \frac{C_p^s}{C_r^s}$$

(3)

C_p^s - Concentration of feed solute in Permeate

C_r^s - Concentration of feed solute in Retentate

Variation of solute concentration with respect to time

The solute mass balance in the retentate resulted the variation of solute concentration in the retentate with time as –

$$V_r \frac{dC_r^s}{dt} = V_w A R_v (C_r^s - C_{p,f}^s)$$

(4)

C_{p,f}^s - concentration of either RHL monomers or insolubilized CV in aqueous phase

➤ In case of RHL

It was assumed that there was no variation in the rejection of RHL vesicles with time. The concentration of RHL in the aqueous phase was assumed to be constant at its CMC value -

$$C_{p,f}^s = \text{CMC}$$

The equation becomes -

$$V_r \frac{dC_r^{\text{RHL}}}{dt} = V_w A R_v (C_r^{\text{RHL}} - \text{CMC})$$

➤ **In case of CV**

The concentration of Crystal Violet in the aqueous phase could be expressed in terms of RHL vesicle binding constant (K_{RHL}^{CV}) as –

$$C_{p,f}^{CV} = \frac{C_r^{CV}}{1 + K_{RHL}^{CV} \times (C_r^{RHL} - CMC)}$$

The equation becomes –

$$V_r \frac{dC_r^{CV}}{dt} = V_w A R_v \left(C_r^{CV} - \frac{C_r^{CV}}{1 + K_{RHL}^{CV} (C_r^{RHL} - CMC)} \right) \quad (4)$$

Flux Decline

In the process of MEUF, the feed solution flows perpendicular toward the surface of the membrane. However, with time, there is a gradual change in the flux values caused due to fouling of the membrane. This membrane fouling was assumed to start with the adsorption of solutes and pore blocking followed by the cake layer formation by the CV-RHL aggregates over the membrane. To investigate this flux decline behavior, we used resistance-in-series model coupled with Hermia's cake filtration model for the entire duration of the experiment. The resistance-in-series model considered both fouling mechanisms as well as it accounted the resistance due to adsorption-pore blockage (up to transition time, t_1) and the resistance caused by the cake layer formation (beyond t_1).

➤ **When $t < t_1$**

The initial flux decline ($t \leq t_1$) was due to membrane fouling which was assumed to be started with the adsorption of CV-RHL aggregates onto the surface, and the membrane pore blocking. The time variation of permeate flux was expressed using the phenomenological equation as –

$$V_w = \frac{\Delta P}{\mu(R_m + R_F)}$$

(4)

R_m – Membrane hydraulic resistance

R_F – Fouling resistance caused by adsorption of CV

ΔP – Operating Pressure

It was observed that in the presence of stirring, the fouling resistance increased with time but at a decreasing rate, reaching a maximum value at the transition time (onset of cake formation). Thus the rate of growth of adsorption-pore blocking fouling resistance could be expressed a

$$R_F = R_{FM} [1 - \exp(-K_1 t)]$$

R_{FM} – Max Fouling resistance

K_1 – kinetic parameter, indicates the growth rate of adsorption-pore blocking fouling resistance

➤ **When $t > t_1$**

It was assumed that the formation of the cake layer started after the completion of solute adsorption and pore blocking. Hermia's cake filtration model for dead-end filtration was coupled with resistance-in-series model. Hence, the equation becomes –

$$V_w = \frac{\Delta P}{\mu [R_m + R_F(t_1) + R_C(t - t_1)]} \quad (2)$$

R_c – Cake Resistance
 $R_F(t_1)$ – Fouling Resistance at $t = t_1$
 μ – Viscosity of permeate

The resistance due to the cake layer formation can be calculated as –

$$R_c = \frac{\alpha(C_o - CMC)V_p}{A}$$

α – Specific Cake Resistance
 C_o – Concentration of retentate at $t = 0$
 V_p – Volume of Permeate

The volume of permeate, V_p , is depends on the change in time. We can calculate it alongside on finding the changes in the volume of retentate with respect to time.

$$V_p(t) = V_o - V_r(t)$$

Therefore, we can find the cake resistance at each time interval by –

$$R_c(t) = \frac{\alpha(C_o - CMC)(V_o - V_r(t))}{A}$$

➤ **Specific Cake Resistance**

The average specific cake resistance (α) is often used to characterize the hydrodynamic resistance of cakes during the MEUF. This gives a measure of the resistance offered by the deposited layer for its flow.

It depends on particle size, shape, density and porosity of the cake and depends on the pressure.

$$\alpha = \alpha_o(\Delta P)^n$$

α_o – Specific resistance at unit pressure
 n – Compressibility factor

If $n = 0$, the deposited layer is incompressible. Generally, its value lies between [0.4,0.8]

With increase in pressure, the porosity of the cake decreases and specific cake resistance increases. This shows the compressibility of the cake.

$$R_c = \alpha^*(1 - \epsilon_p) * \rho_g * L$$

$$\alpha = \frac{180(1 - \epsilon_p)}{D_p^2 \epsilon_p^2 \rho_g}$$

ϵ_p – Void Fraction
 ρ_g – Density of Cake
 D_p – Diameter of deposited solute

PROCEDURE

The three model parameters namely, α , ΔP , and R_v were estimated through an optimization method and by minimizing the sum of square errors between the calculated and experimental data of permeate flux and permeate concentration. On using the values of the optimized model parameters, the performance of the MEUF experiments was predicted. The complete analysis was done using MATLAB.

1. For stage 1 ($t < t_1$), the permeate flux values, retentate volume, retentate concentration and permeate the concentration at various operation time were calculated by solving the coupled differential and algebraic equations with the following initial condition, at $t = 0$, $Cr^s = C_0$, and $V_r = V_0$.
2. Then, the time was increased to $t + \Delta t$. It was repeated till $t = t_1$
3. For stage 2 ($t > t_1$), the permeate flux, retentate volume, retentate concentration and permeate the concentration at various operation times were calculated by solving the coupled differential and algebraic equations with the initial condition, at $t = t_1$, $R_c = 0$, $Cr^s = Cr^s(t_1)$ and $V_r = V_r(t_1)$.
4. The time (t) was increased to $t + \Delta t$ next. It was repeated till $t = t_i$
5. The sum of square errors between the calculated and experimental values of permeate flux and permeate concentration were calculated for the entire duration of the experiment. The sum of square errors was defined as –

$$E = \sum_{i=1}^N \left(\frac{V_{w,i}^{exp} - V_{w,i}^{cal}}{V_{w,i}^{exp}} \right)^2$$

N is the number of experimentally measured data points

6. If $E \leq 0.01$, the program was terminated. The desire corresponding values of α , ΔP , and R_v were recorded. Thus, the transient profiles of permeate flux, retentate volume, solute concentration in retentate and permeate were obtained. The model was validated by comparing the calculated values of permeate flux and permeate concentrations with those observed during experiments.

CLEANING OF MEMBRANE

After the experiment, the cell was dismantled and the membrane was taken off from the cell carefully and washed with distilled water followed by static chemical cleaning at room temperature. Clean the membrane with an aqueous HCl solution (pH 3.0) for 15 min. Rinse it with distilled water for 15 min. Clean it with an aqueous NaOH solution (pH 10.0) for 15 min. The membrane was again washed with distilled water. Then, the cell was reassembled and the membrane permeability was checked using distilled water.

VARIOUS PARAMETRIC VALUES

- ❖ Effective Membrane Area, $A = 37.5 * 10^{-4} \text{ m}^2$
- ❖ Critical Micelle Concentration, $\text{CMC} = 50 * 10^{-3} \text{ Kg/m}^3$
- ❖ Membrane Permeability, $L_p = 4.7 * 10^{-11}$
- ❖ Membrane Hydraulic Resistance, $R_m = 21 * 10^{12} \text{ m}^{-1}$
- ❖ Transient time, $t_1 = 300 \text{ sec}$
- ❖ Membrane Fouling Resistance, $R_{FM} = 7.6 * 10^{12} \text{ m}^{-1}$
- ❖ Final operating time, $t_t = 3600 \text{ sec}$
- ❖ Kinetic Parameter, $K_1 = 1.08 * 10^{-2} \text{ sec}^{-1}$
- ❖ Cake Filtration Constant, $K_c = 2 * 10^5 \text{ sec/m}^2$
- ❖ RHL Vesicle Binding Constant, $K_{cv} = 27 \text{ m}^3/\text{kg}$
- ❖ Viscosity of water, $\mu = 10^{-3} \text{ Kg/m}^3$

Initial Guess Values of Model Parameters

- ❖ Operating Pressure, $P = 276 \text{ kPa}$
- ❖ Specific Cake Resistance, $\alpha = 8 * 10^{15} \text{ m/kg}$
- ❖ Rejection rate of RHL Vesicles, $R_v = 0.99$

At the time, $t = 0$

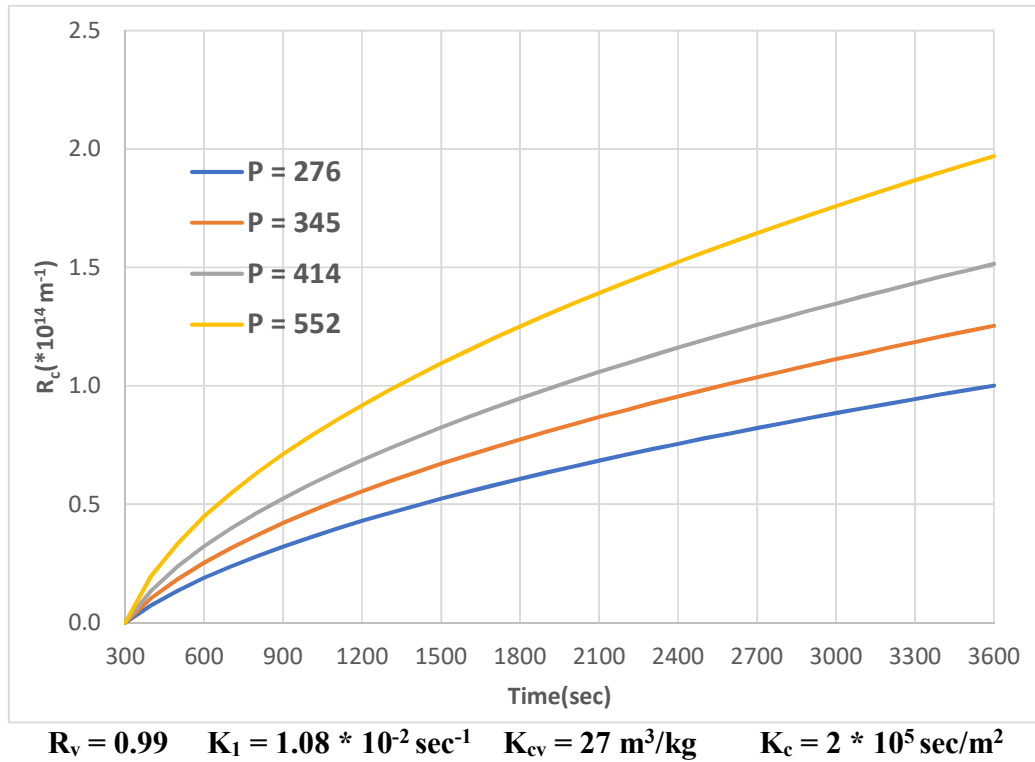
- ❖ Initial volume of permeate, $V_o^p = 0.1 * 10^{-3} \text{ m}^3$
- ❖ Initial Concentration of Crystal Violet, $C_o^{CV} = 30 * 10^{-3} \text{ kg/m}^3$
- ❖ Initial Concentration of Rhamnolipid, $C_o^{RHL} = 1 \text{ Kg/m}^3$

For Experimental Calculations

- ❖ Volume of Feed, $V_o = 150 \text{ mL}$
- ❖ Volume of Permeate, $V_p = 75 \text{ mL}$
- ❖ Volume of Retentate, $V_r = 150 - 75 = 75 \text{ mL}$
- ❖ Volume Concentration Ratio, $V_{cr} = 150/75 = 2$
- ❖ Rotation Per Min of stirrer, $\omega = 500 \text{ rpm}$

RESULT AND DISCUSSION

➤ R_c (m^{-1}) vs Time (sec) at different pressures

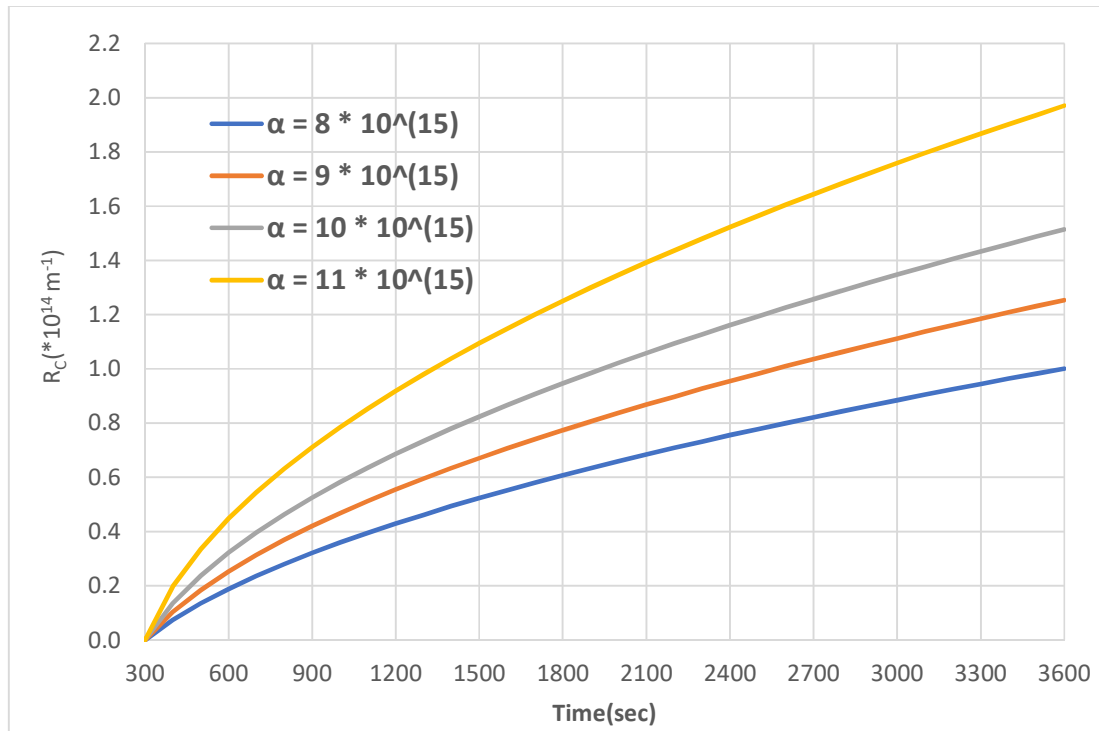


This graph shows the variation of cake layer resistance with time at various operating pressures. This cake layer started forming after a particular time and continued to form since then. It is observed that there is a gradual increase in cake layer resistance with time. All the other parameters are kept constant. Also, with an increase in pressure there is a more significant variation in the Cake Layer Resistance. On increasing the value of operating pressure, there is a higher amount of resistance caused by the formation of cake layer.

At $t = 1800 \text{ sec}$

P (kPa)	276	345	414	552
$R_c (*10^{14} \text{ m}^{-1})$	0.6075	0.7740	0.9468	1.2504

➤ $R_c(m^{-1})$ vs Time(sec) at different specific cake resistances



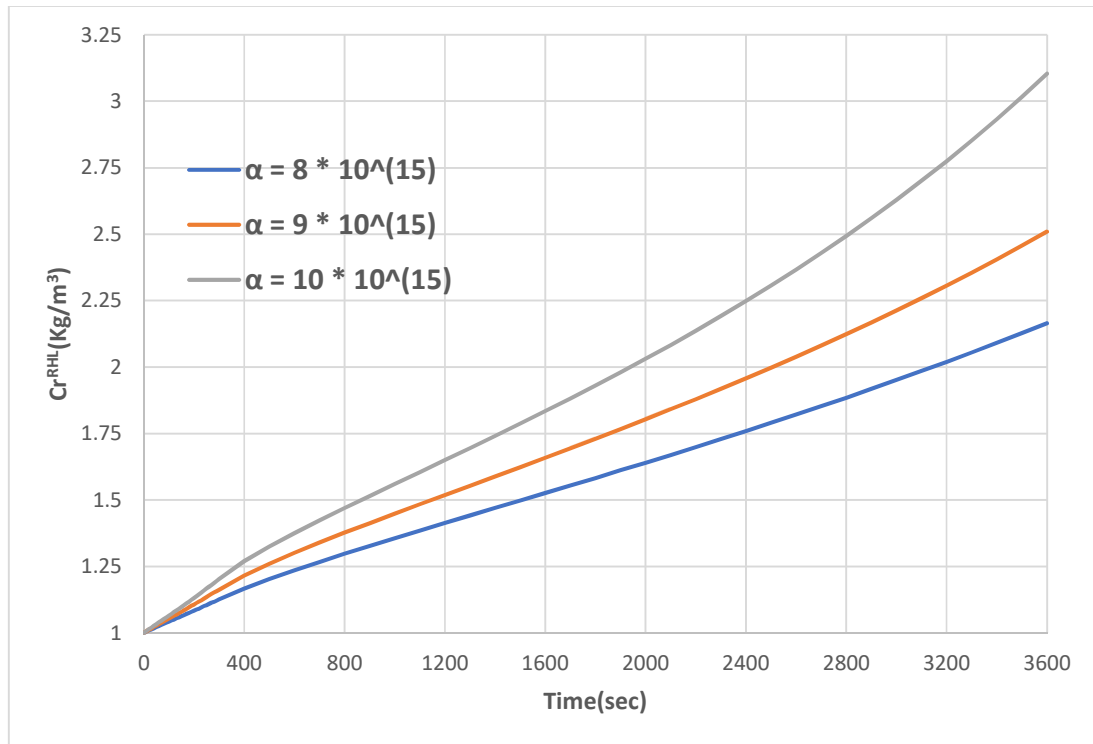
$$R_v = 0.99 \quad K_1 = 1.08 \times 10^{-2} \text{ sec}^{-1} \quad K_{cv} = 27 \text{ m}^3/\text{kg} \quad K_c = 2 \times 10^5 \text{ sec/m}^2$$

This graph shows the variation of cake layer resistance with time at various specific cake layer resistances. This cake layer started forming after a particular time and continued to form since then. It is observed that there is a gradual increase in cake layer resistance with time. All the other parameters are kept constant. Also, with an increase in specific cake layer resistance, there is a more significant variation in the Cake Layer Resistance. On increasing the value of specific cake layer resistance, there is a higher amount of resistance caused by the formation of cake layer.

At $t = 1800 \text{ sec}$

$\alpha(*10^{15} \text{ m/kg})$	8	9	10	11
$R_c(*10^{14} \text{ m}^{-1})$	0.6075	0.7740	0.9468	1.2504

➤ $Cr^{RHL}(\text{Kg}/\text{m}^3)$ vs Time(sec) at specific cake resistances



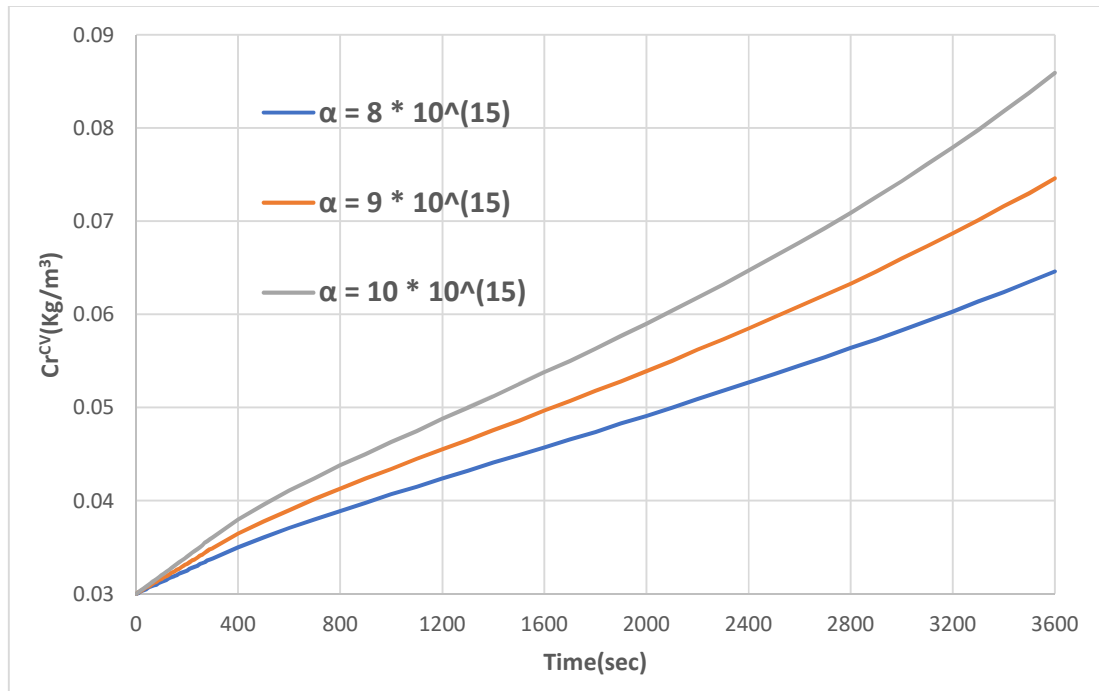
$$R_v = 0.99 \quad K_1 = 1.08 * 10^{-2} \text{ sec}^{-1} \quad K_{cv} = 27 \text{ m}^3/\text{kg} \quad K_c = 2 * 10^5 \text{ sec}/\text{m}^2$$

This graph shows the variation of concentration of Rhamnolipid with time at various specific cake layer resistances. It is observed that there is a gradual increase in concentration of Rhamnolipid with increasing time. All the other parameters are kept constant. Also, with an increase in specific cake layer resistance, initially the concentrations of the Rhamnolipid are constant. However, after a certain time, there is a more significant variation in the Cake Layer Resistance. The variation of concentration of Rhamnolipid with time is higher with higher values of specific cake layer resistance.

At $t = 1800$ sec

$\alpha(*10^{15} \text{ m}/\text{kg})$	8	9	10
$Cr^{RHL}(\text{Kg}/\text{m}^3)$	1.5826	1.7302	1.9306

➤ $C_r^{CV}(\text{Kg/m}^3)$ vs Time(sec) at specific cake resistances



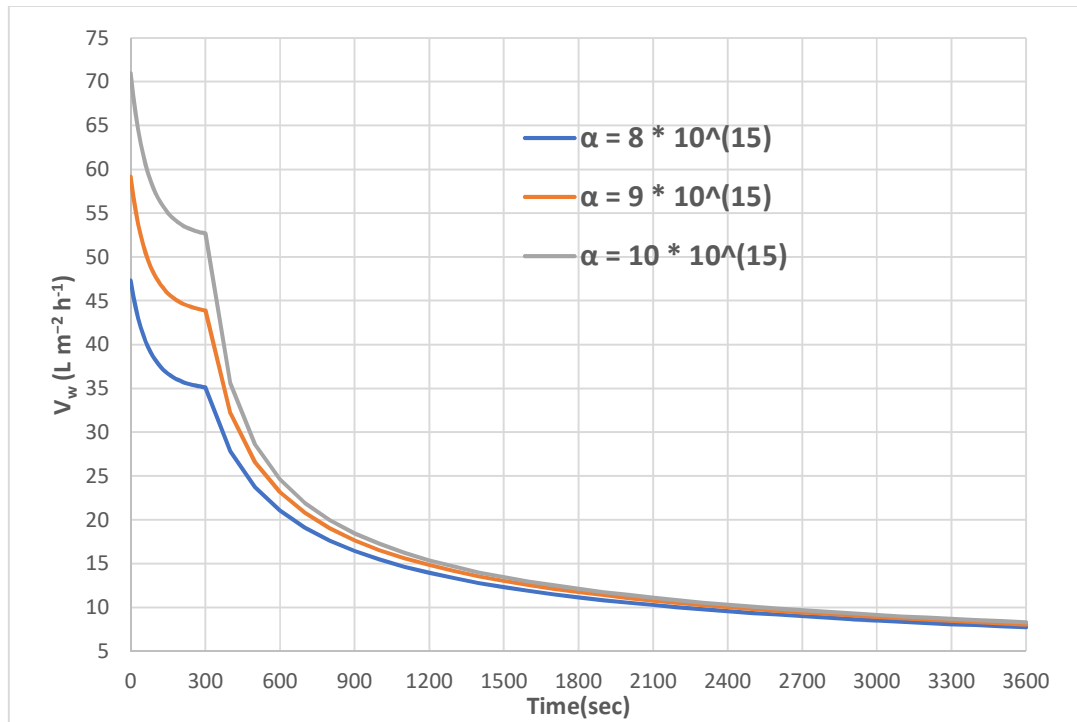
$R_v = 0.99$ $K_1 = 1.08 * 10^{-2} \text{ sec}^{-1}$ $K_{cv} = 27 \text{ m}^3/\text{kg}$ $K_c = 2 * 10^5 \text{ sec/m}^2$

This graph shows the variation of concentration of Crystal Violet with time at various specific cake layer resistances. It is observed that there is a gradual increase in concentration of Crystal Violet with increasing time. All the other parameters are kept constant. Also, with an increase in specific cake layer resistance, initially the concentrations of the Crystal Violet are constant. However, after a certain time, there is a more significant variation in the Cake Layer Resistance. The variation of concentration of Crystal Violet with time is higher with higher values of specific cake layer resistance.

At $t = 1800 \text{ sec}$

$\alpha (*10^{15} \text{ m/kg})$	8	9	10
$C_r^{CV}(\text{Kg/m}^3)$	0.0474	0.0518	0.0563

➤ V_w ($L m^{-2} h^{-1}$) vs time(sec) at specific cake resistances



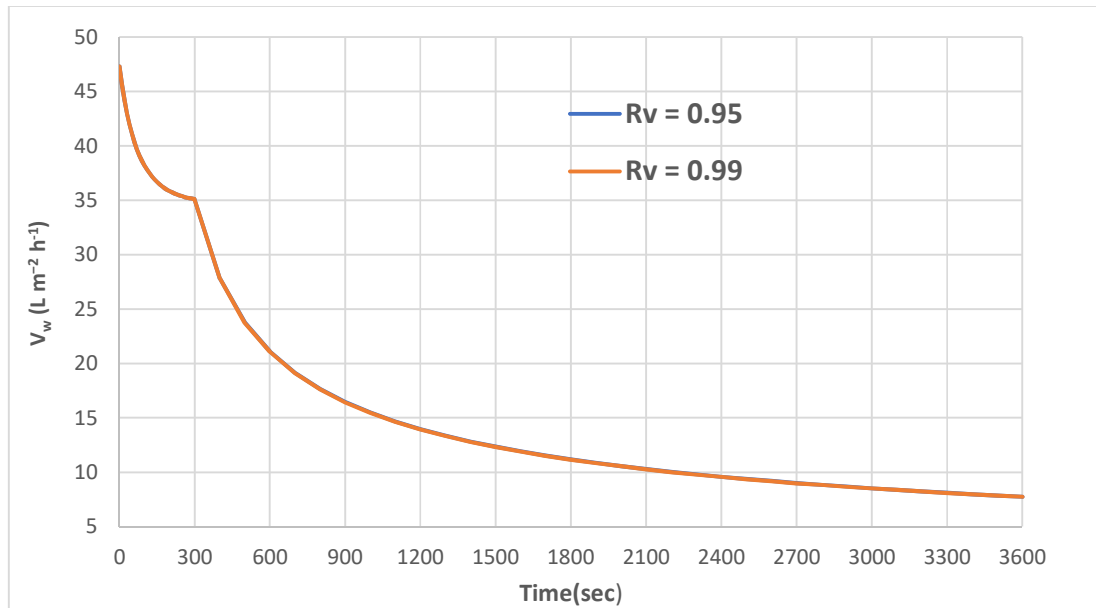
$$R_v = 0.99 \quad K_1 = 1.08 * 10^{-2} \text{ sec}^{-1} \quad K_{cv} = 27 \text{ m}^3/\text{kg} \quad K_c = 2 * 10^5 \text{ sec/m}^2$$

This graph shows the variation of permeate flux with time at various specific cake layer resistances. It is observed that there is a gradual decrease in the permeate flux up to a certain time. However, after this transient time, when the cake is formed, initially there is a greater rate of decline in permeate flux. But after sometime, the rate of decline in flux does not have a very significant variation. All the other parameters are kept constant. Also, with an increase in specific cake layer resistance, there is an increase in the rate of declining permeate flux. However, after the transient time, the decline permeate flux values comes closer and there is not much difference in the values after some time.

At $t = 1800 \text{ sec}$

$\alpha (*10^{15} \text{ m/kg})$	8	9	10
$V_w (L m^{-2} h^{-1})$	11.1600	11.7360	12.1320

➤ $V_w(\text{L m}^{-2} \text{h}^{-1})$ vs time(sec) at different RHL rejection rates



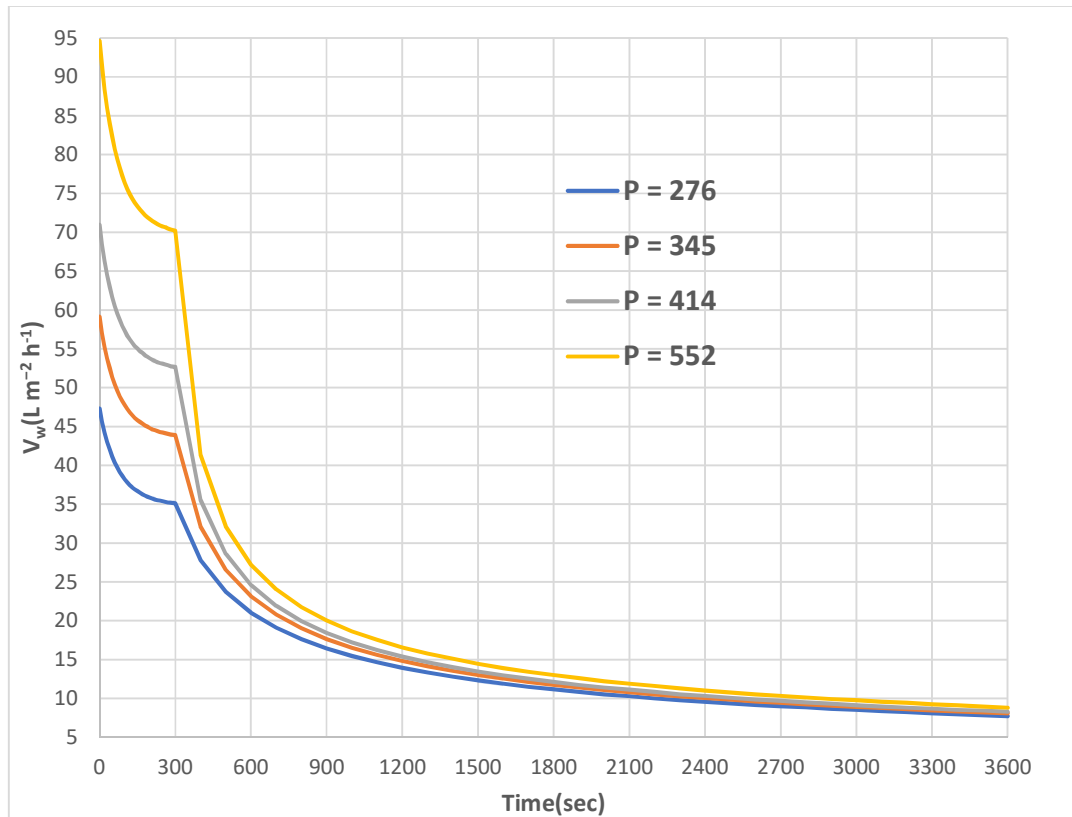
$P = 276 \text{ kPa}$ $K_1 = 1.08 * 10^{-2} \text{ sec}^{-1}$ $K_{cv} = 27 \text{ m}^3/\text{kg}$ $K_c = 2 * 10^5 \text{ sec}/\text{m}^2$

This graph shows the variation of permeate flux with time at different rejection rates of RHL Vesicles. It is observed that there is a gradual decrease in the permeate flux up to a certain time. However, after this transient time, when the cake is formed, initially there is a greater rate of decline in permeate flux. But after sometime, the rate of decline in flux does not have a very significant variation. All the other parameters are kept constant. Also, with an increase in Rejection rate of RHL Vesicles, we can see that there is no variation in the permeate flux values. However, after some time, there is a very slight decrement in the rate of declining permeate flux.

At $t = 1800 \text{ sec}$

R_v	0.95	0.99
$V_w (\text{L m}^{-2} \text{h}^{-1})$	11.1821	11.1568

➤ $V_w(\text{L m}^{-2} \text{h}^{-1})$ vs time(sec) at different pressures



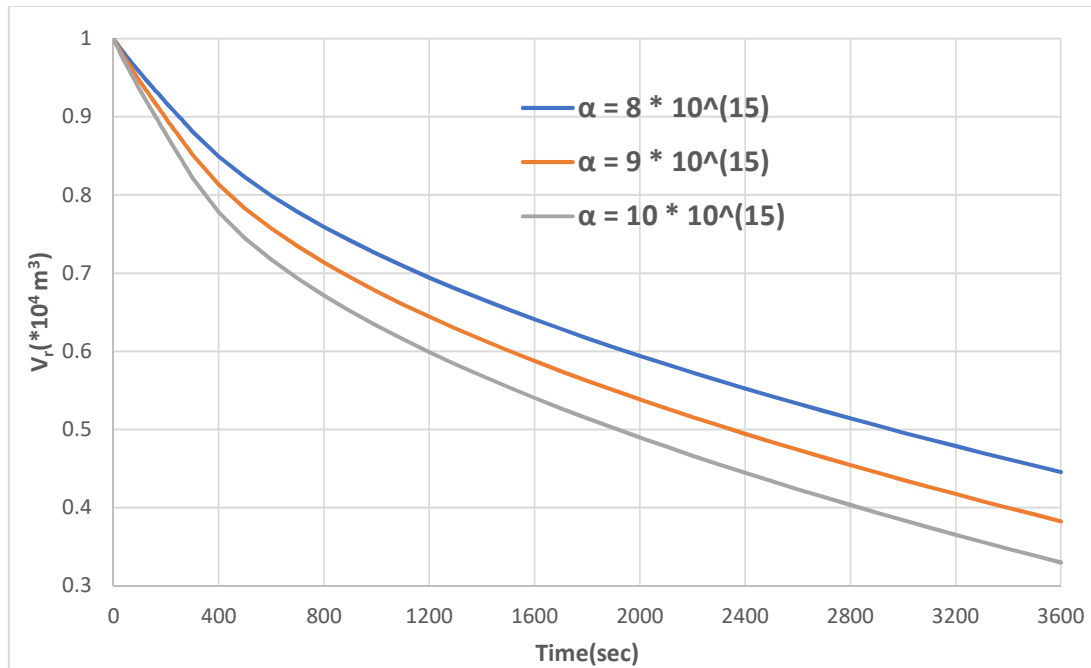
$$R_v = 0.99 \quad K_1 = 1.08 \times 10^{-2} \text{ sec}^{-1} \quad K_{cv} = 27 \text{ m}^3/\text{kg} \quad K_c = 2 \times 10^5 \text{ sec/m}^2$$

This graph shows the variation of permeate flux with time at various operating pressures. It is observed that there is a gradual decrease in the permeate flux up to a certain time. However, after this transient time, when the cake is formed, initially there is a greater rate of decline in permeate flux. But after sometime, the rate of decline in flux does not have a very significant variation. All the other parameters are kept constant. Also, with an increase in operating pressure, there is an increase in the rate of declining permeate flux. However, after the transient time, the decline permeate flux values tends to come closer and there is not much difference in the values after some time.

At $t = 1800 \text{ sec}$

P (kPa)	276	345	414	552
$V_w(\text{L m}^{-2} \text{h}^{-1})$	11.1568	11.7498	12.1189	12.9840

➤ $V_r(\text{m}^3)$ vs Time(sec) at different specific cake resistances



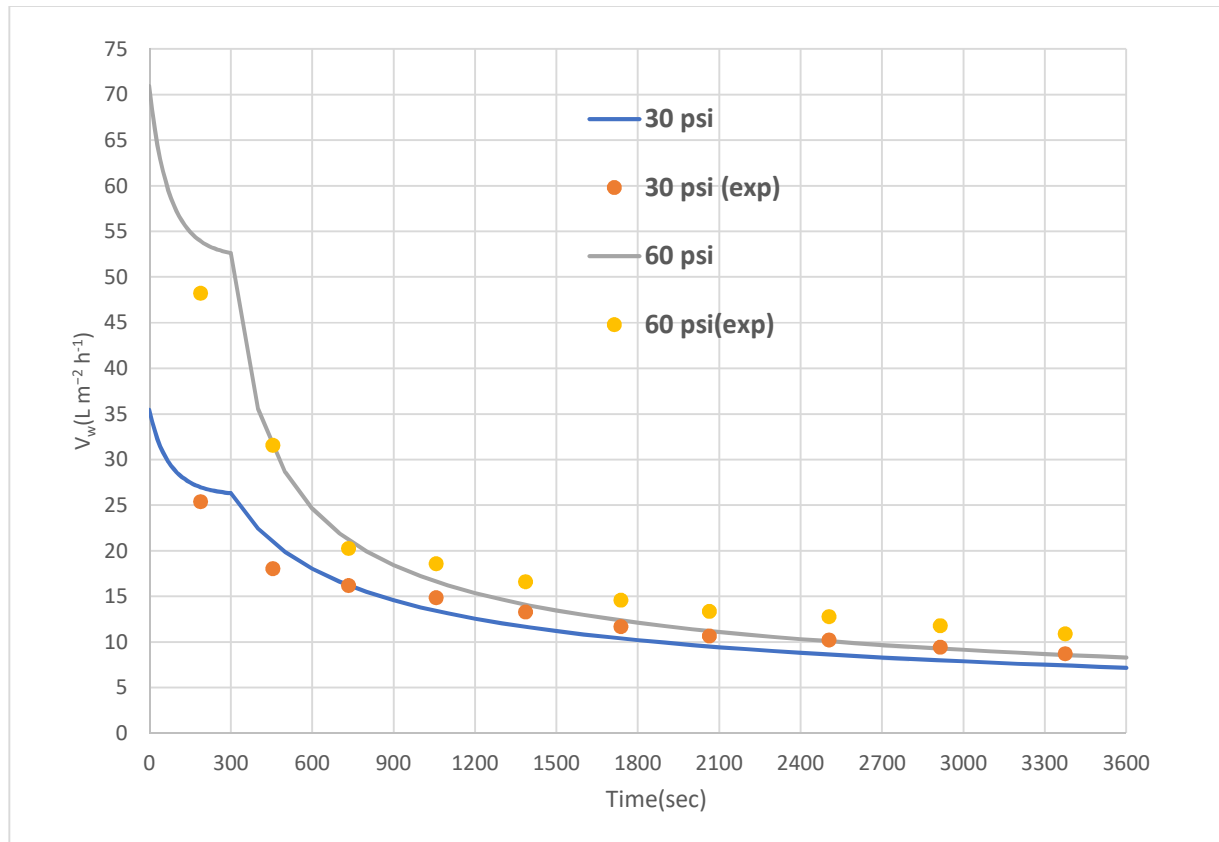
$R_v = 0.99$ $K_1 = 1.08 * 10^{-2} \text{ sec}^{-1}$ $K_{cv} = 27 \text{ m}^3/\text{kg}$ $K_c = 2 * 10^5 \text{ sec/m}^2$

This graph shows the variation of volume of permeate with time at various specific cake layer resistances. It is observed that there is a gradual decrease in the volume of permeate with increasing time. All the other parameters are kept constant. Also, with an increase in specific cake layer resistance, there is a more significant variation in the Cake Layer Resistance. The variation of volume permeate with time is higher with higher values of specific cake layer resistance.

At $t = 1800$

$\alpha (*10^{15} \text{ m/kg})$	8	9	10
$V_r (*10^4 \text{ m}^3)$	0.6169	0.5622	0.5143

Experimental Interpretation



$$\omega = 500 \text{ rpm} \quad R_v = 0.99 \quad K_1 = 1.08 \times 10^{-2} \text{ sec}^{-1} \quad K_{cv} = 27 \text{ m}^3/\text{kg} \quad K_c = 2 \times 10^5 \text{ sec}/\text{m}^2$$

This graph shows the variation of permeate flux with time at various operating pressures. Here, we compared the experimental readings along with the analyzed readings at the same operating pressures. The experiment was conducted at two different operating pressures –

- $P_1 = 30 \text{ psi} = 206.843 \text{ kPa}$
- $P_2 = 60 \text{ psi} = 413.685 \text{ kPa}$

For experimental interpretations, continuous flux readings were taken at a fixed volume interval till a desired volume of permeate is recovered. It was observed that the time difference increased with more volume of permeate coming out of the stirred cell. However, after sometime, the time difference and the corresponding flux values were nearly constant. The experimental readings and the analyzed readings are very close to each other.

CONCLUSION

A dye is a substance that is used to impart color to textiles, cosmetics, paper, leather, rubber and other materials. With the increasing number textile, sugar, paper industries, the usage of dyes has also increased considerably. The industries tend to dump the dyes into water bodies which creates hazardous effects to the environment. They are highly soluble in water and have acidic and toxic nature. Hence, it is need of an hour to remove these dyes from the wastewater.

Micellar-Enhanced Ultrafiltration was used to investigate continuous removal of highly used Crystal Violet dye from aqueous solution using the bio surfactant Rhamnolipid. The experiment was done using a stirred cell batch membrane set up. To get analysis of permeate flux decline at certain operating conditions, a model was developed using MATLAB. The detailed parametric study revealed that permeate flux increased with an increase in transmembrane pressure difference and also increased with increase in specific cake layer resistance. However, it did not show any significant impact with a change in the rejection rate of RHL.

Using the estimated model parameters, the model successfully predicted the profiles of permeate flux, cake layer resistance, retentate concentration, Rhamnolipid concentration and volume of permeate at certain conditions. The predominant fouling mechanism was caused by the formation of cake layer. This cake layer was responsible for adsorption-pore blocking. Operating conditions showed a significant influence on the transition time of the fouling mechanism.

For experimental interpretations, continuous flux readings were taken at a fixed volume interval till a desired volume of permeate is recovered. It was observed that the time difference increased with more volume of permeate coming out of the stirred cell. However, after sometime, the time difference and the corresponding flux values were nearly constant. The experimental readings and the analyzed readings are very close to each other.

REFERENCES

1. Use of Rhamnolipid in micellar-enhanced ultrafiltration for simultaneous removal of Cd⁺² and crystal violet from aqueous solution, Satya Pal Verma | Biswajit Sarkar, <https://doi.org/10.1002/apj.2315>
2. An efficient removal of crystal violet from aqueous solution using Rhamnolipid micellar Solubilization followed by ultrafiltration and modelling of flux decline, Satya Pal Verma, Nikhil Rao Mallela, Biswajit Sarkar, <https://doi.org/10.1016/j.jece.2020.104443>
3. Rhamnolipid based micellar-enhanced ultrafiltration for simultaneous removal of Cd(II) and phenolic compound from wastewater, Satya Pal Verma, Biswajit Sarkar, <https://doi.org/10.1016/j.ccej.2017.03.009>
4. Analysis of flux decline during Rhamnolipid based micellar-enhanced ultrafiltration for simultaneous removal of Cd⁺² and crystal violet from aqueous solution, Satya Pal Verma, Biswajit Sarkar, <https://doi.org/10.1016/j.jwpe.2019.101048>
5. Simultaneous removal of Cd (II) and p-cresol from wastewater by micellar-enhanced ultrafiltration using Rhamnolipid: Flux decline, adsorption kinetics and isotherm studies, Satya Pal Verma, Biswajit Sarkar, <https://doi.org/10.1002/apj.2315>
6. Use of Rhamnolipid to remove heavy metals from wastewater by micellar-enhanced ultrafiltration (MEUF), M.A. Monem, El Zeftawy, Catherine N.Mulligan, <https://doi.org/10.1016/j.seppur.2010.11.030>
7. Adsorption of hazardous dye crystal violet from wastewater by waste materials, Alok Mittala, Jyoti Mittala, Arti Malviyaa, Dipika Kaur, V.K. Gupta, <https://doi.org/10.1016/j.jcis.2009.11.060>
8. Removal of dye from wastewater using micellar-enhanced ultrafiltration and recovery of surfactant, M.K Purkait, S Das Gupta, S De, <https://doi.org/10.1016/j.seppur.2003.08.005>